Modeling and Autopilot Design of Blended Wing-Body UAV

Byoung-Mun Min*
Department of Aerospace Engineering, School of Mechanical, Aerospace & Systems Engineering, KAIST, Daejeon, Korea 305-701

Sung-Sik Shin**
UAV Group, Korea Institute of Aerospace Technology, Korean Air, Daejeon, Korea 305-811

Hyunchul Shim* and Min-Jea Tahk******
Department of Aerospace Engineering, School of Mechanical, Aerospace & Systems Engineering, KAIST, Daejeon, Korea 305-701

Abstract

This paper describes the modeling and autopilot design procedure of a Blended Wing-Body(BWB) UAV. The BWB UAV is a tailless design that integrates the wing and the fuselage. This configuration shows some aerodynamic advantages of lower wetted area to volume ratio and lower interference drag as compared to conventional type UAV. Also, BWB UAV may be increase payload capacity and flight range. However, despite of these benefits, this type of UAV presents several problems related to flying qualities, stability, and control. In this paper, the detailed modeling procedure of BWB UAV and stability analysis results using the linearized model at trim condition are represented. Finally, we designed the autopilot of BWB UAV based on a simple control allocation scheme and evaluated its performance through nonlinear simulation.

Key Word : Blended Wing-Body(BWB) UAV, Tailless, Modeling procedure, Stability analysis, Autopilot, Control allocation, Performance, Nonlinear simulation

Introduction

Initially, BWB configuration has been proposed to improve the economic efficiency of future air transportation [1,2]. The BWB is sometimes referred to a 'flying wing' due to its configuration of the integrated wing and fuselage as lifting surface. It is a revolutionary conceptual change from the conventional aircraft of which wing is attached to a cylindrical fuselage with a vertical tail to ensure the directional stability and maneuverability. Conceptually, since BWB configuration possesses lower wetted area to volume ratio and lower interference drag compared to the conventional type of aircraft, it may increase the maximum lift-to-drag ratio $(L/D)_{max}$ to about 20% over the conventional design. These aerodynamic advantages can be obtained by an optimized aerodynamic shape. Hence, a number of researches on BWB configuration are only focused on the aerodynamic study and the determination of a detailed shape design [3-6]. Also, a BWB UAV shows lower stall speed in comparison to the conventional fixed-wing UAV without flap. Because of this flight characteristics, BWB UAV

* Ph.D Student
** Senior Researcher
*** Assistant Professor
**** Professor
E-mail : mjtahk@fdcl.kaist.ac.kr Tel : 042-869-3718 FAX : 042-869-3710

may reduce the impulse at the moment of recovering it using a net. Nevertheless, these significant benefits over conventional design, stability and control problems are still remained as the main drawback of BWB configuration [7]. In the aspect of stability, longitudinal static stability is assured when the aerodynamic center, i.e. *a.c*, of the wing is located behind of the center of gravity, i.e. *c.g*. However, unfortunately *a.c* of BWB UAV is very closely located to its *c.g* or sometimes *a.c* is located ahead of *c.g*. Also, BWB UAV inherently shows very low directional stability and adverse yaw characteristics during rolling maneuver because there is no rudder to counteract the adverse yaw [2]. About the longitudinal dynamics of BWB UAV, it was founded that the short period mode reveals shorter periods and slightly less damped than comparable conventional types [8]. Also, due to a revolutionary configuration of BWB UAV, it has much shorter pitching moment arm than conventional type of fixed-wing UAV. This fact causes the problem that BWB UAV may do not occasionally generate the sufficient pitching moment for vertical maneuver. Moreover, since the right and left control surfaces simultaneously practice the longitudinal and the lateral-directional motions, control allocation scheme is necessarily implied to flight control system of BWB UAV.

In this paper, we construct a detailed dynamic model of BWB UAV to investigate its flight performance and analysis its stability. Using this dynamic model, autopilot for a BWB UAV is designed by applying a simple control allocation scheme and its control performance is evaluated through nonlinear simulation.

Modeling of BWB UAV

A BWB UAV adopted for this research features a pure 'blended wing-body' configuration as shown in Fig. 1 and its some physical parameters are summarized in Table 1. As shown in Fig. 1, there is only two control surfaces attached to the trailing edge of right and left wings. It has two vertical panels at the both side of wing tip to enhance the directional stability. A 30*amps* and 11*volts* brushless motor is mounted at the end of the fuselage and 12×6 propeller is used.

Equation of motion

The 6-DOF equations of motion of BWB UAV can be expressed in the same manner of conventional aircraft under the assumption of the flat Earth and constant mass properties. Thus, the translational and rotational motion of BWB UAV can be written as follows:

Table 1. Physical Parameters of BWB UAV

Weight	empty	1.2	kg	including battery and motor		
	total	2.5		including FCC and navigation sensors		
Moment of inertia	I_{xx}	0.1080	kg · m2	Wing span	1.52	m
	I_{yy}	0.0423		Wing area	0.554	m2
	I_{zz}	0.1361		Mean aerodynamic chord	0.29	m

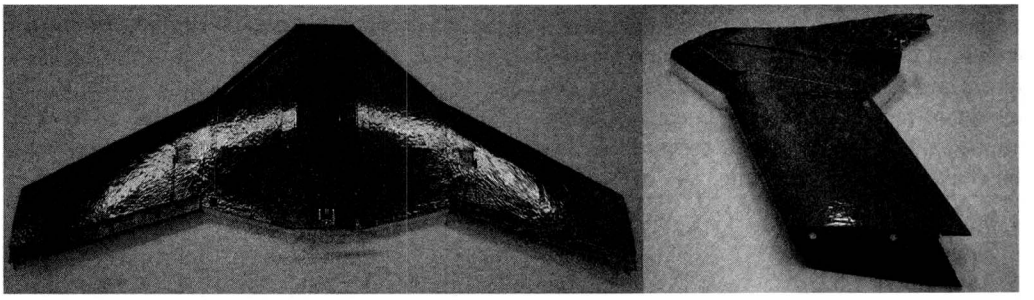

Fig. 1. Configuration of Blended Wing-Body(BWB) UAV

$$\begin{aligned}
\dot{U} &= RV - QW - g_0 \sin\theta + F_x/m \\
\dot{V} &= -RU + PW + g_0 \sin\phi\cos\theta + F_y/m \\
\dot{W} &= QU + PV + g_0 \cos\phi\cos\theta + F_z/m
\end{aligned} \tag{1}$$

$$\begin{aligned}
\dot{P} &= (c_1 R + c_2 P)Q + c_3 L + c_4 N \\
\dot{Q} &= c_5 PR - c_6 (P^2 - R^2) + c_3 M \\
\dot{R} &= (c_8 P - c_2 R)Q + c_4 L + c_9 N
\end{aligned} \tag{2}$$

where the notations and the definitions of c_1 to c_9 in Eqs. (1) and (2) are referred to Ref. [9].

Aerodynamic modeling

External forces and moments are the most significant factor to ensure the modeling fidelity of considering platform. Among the three external force and moment sources, i.e. aerodynamic effect , engine thrust, and gravity, aerodynamic force and moment are the more important component determining the flying quality of a BWB UAV. Aerodynamic coefficients are usually obtained from extensive theoretical and experimental works such as CFD analysis, wind tunnel test, and flight test. In this research, non-dimensional aerodynamic static and dynamic stability derivatives are calculated by using the software of 'Digital DATCOM'. 'Digital DATCOM' calculates static stability, high-lift and control device, and dynamic-derivative characteristics using the geometric data as shown in Fig. 2. It also offers a trim option that computes control deflections and aerodynamic data for vehicle trim at subsonic Mach numbers [10].

Figs. 3 and 4 illustrate some static stability and control derivatives calculated by 'Digital DATCOM'. In the BWB UAV considered in this research, only one pair of control surface as shown in Fig. 2 is actuated as an elevon, i.e. right and left control surfaces are deflected in the same direction for pitch control and deflected in the opposite direction for roll control. We can observe from Fig. 4 that pitching moment effect is about 10 times larger than roll moment effect by deflecting the control surface. The reason is caused by the fact that the wing of this BWB UAV is attached with a comparatively large sweepback angle to obtain a sufficient moment arm and its configuration has the reduced kinematic damping in the pitch direction. Finally, the relation between the stability derivatives and force and moment coefficients for this BWB UAV can be expressed as follows:

$$\begin{aligned}
C_L^{Total} &= C_L(M,\alpha) + C_{L_a}(M,\alpha) + \left(\frac{1}{2}\Delta_{ev} C_D\left(M,\delta_{ev}^R\right) + \frac{1}{2}\Delta_{ev} C_D\left(M,\delta_{ev}^L\right)\right) \\
&\quad + \frac{\bar{c}}{2V_T} C_{L_q}(M,\alpha)\cdot q \\
C_D^{Total} &= C_D(M,\alpha) + \left(\frac{1}{2}\Delta_{ev} C_D\left(M,\delta_{ev}^R\right) + \frac{1}{2}\Delta_{ev} C_D\left(M,\delta_{ev}^L\right)\right) \\
C_Y^{Total} &= C_{Y_\beta}(M)\cdot\beta + \frac{b}{2V_T}\left(C_{Y_p}(M,\alpha)\cdot p + C_{Y_r}(M,\alpha)\cdot r\right)
\end{aligned} \tag{3}$$

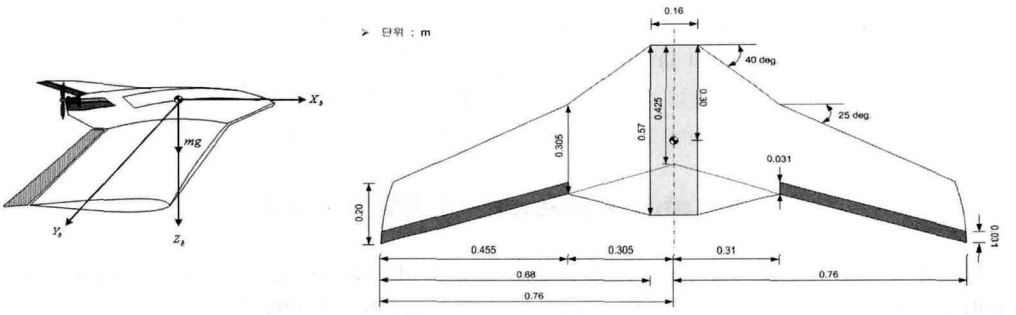

Fig. 2. Geometric Data of BWB UAV for Digital DATCOM

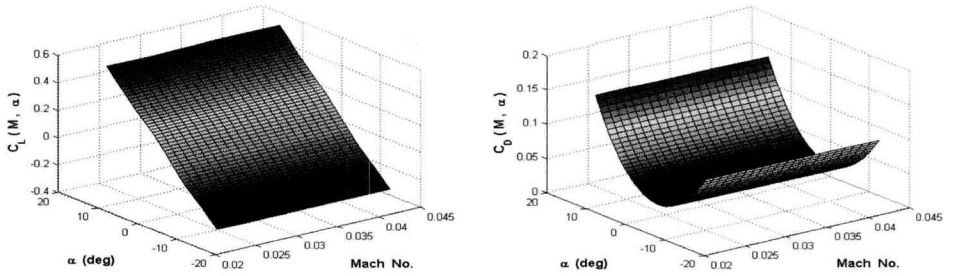

Fig. 3. Static Stability Derivatives : Lift and Drag Coefficients

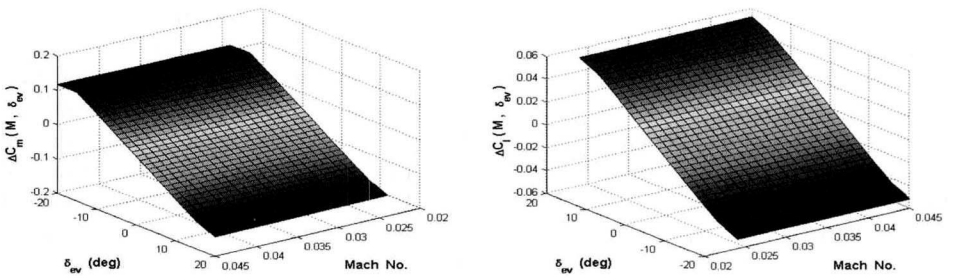

Fig. 4. Control Derivatives : Incremental Pitching and Rolling Moment Coefficients w.r.t Control Surface Deflection

$$
\begin{aligned}
C_l^{Total} &= C_{l_\beta}(M,\alpha)\cdot\beta + \left(\frac{1}{2}\Delta_{ev}C_l\left(M,\delta_{ev}^R\right) - \frac{1}{2}\Delta_{ev}C_D\left(M,\delta_{ev}^L\right)\right) \\
&\quad + \frac{b}{2V_T}\left(C_{l_p}(M,\alpha)\cdot p + C_{l_r}(M,\alpha)\cdot r\right) \\
C_M^{Total} &= C_M(M,\alpha) + C_{M_\alpha}(M,\alpha) + \left(\frac{1}{2}\Delta_{ev}C_M\left(M,\delta_{ev}^R\right) + \frac{1}{2}\Delta_{ev}C_M\left(M,\delta_{ev}^L\right)\right) \\
&\quad + \frac{\bar{c}}{2V_T}C_{M_q}(M,\alpha)\cdot q + \left(x_{c.g} - x_{c.g}^*\right)\left(C_L^{Total}\cos\alpha + C_D^{Total}\sin\alpha\right) \\
C_N^{Total} &= C_{N_\beta}(M)\cdot\beta + \frac{b}{2V_T}\left(C_{N_p}(M,\alpha)\cdot p + C_{N_r}(M,\alpha)\cdot r\right) \\
&\quad - \left(x_{c.g} - x_{c.g}^*\right)\frac{\bar{c}}{b}C_Y^{Total}\cos\alpha
\end{aligned}
\tag{4}
$$

where δ_{ev}^R and δ_{ev}^L, respectively, denote the deflection angle of the right and left elevon and $x_{c.g}$ and $x_{c.g}^*$ indicate the x-coordinate of the center of gravity and the aerodynamic center . As shown in Eq. (4), if the right and left elevon is deflected in the same direction with the same magnitude, the sum of rolling moment coefficient produced by the elevon deflection, i.e. $\Delta_{ev}C_l$, is zero. On the other hand, if the right and left elevon is deflected in the opposite direction with the same magnitude, the sum of pitching moment coefficient produced by the elevon deflection, i.e. $\Delta_{ev}C_M$, is zero.

Autopilot Design of BWB UAV

Based on the 6-DOF dynamic model described in the above section, we create a nonlinear simulation model for a BWB UAV using Matlab/Simulink. Using this nonlinear simulation modeland 'trim' function which is a built-in function of Matlab/Simulink and solves steady-state

Table 2. Trim Condition of BWB UAV

Flight Condition		Trim State Value		Control Input for Trim Flight	
Speed	12 *m/s*	Angle-Of-Attack	9.14 *deg*	Throttle Level	0.15
Altitude	100 *m*	Flight Path Angle	0.00 *deg*	Elevon Deflection Angle	-2.54 *deg*

Table 3. Dynamic Properties of BWB UAV

Modes		Eigenvalue	Damping Ratio	Natural Frequency
Longitudinal	Short Period	-6.93 ± 12.50j	0.485	14.3 *rad/sec*
	Phugoid	-8.67 ± 1.04j	0.083	1.05 *rad/sec*
Lateral-directional	Dutch-roll	1.14 ± 0.71j	-0.848 (unstable)	1.35
	Roll	-9.20	1.00	9.20
	Spiral	-3.64	1.00	3.64

parameters using a constrained optimization technique, we obtained a trim condition for the steady-state level flight at the altitude of 100 *m* and the speed of 12 *m/s*. Trim condition of BWB UAV at this flight condition is summarized in Table 2. Also, a set of linear equations of motion at this flight condition is obtained. A set of linear longitudinal and lateral-directional dynamics is written as following state-space form.

Longitudinal dynamics

$$\begin{bmatrix} \dot{V}_T \\ \dot{\alpha} \\ \dot{\theta} \\ \dot{q} \\ \dot{h} \end{bmatrix} = \begin{bmatrix} -0.239 & 1.513 & -9.810 & 0.000 & 0.000 \\ -0.133 & -5.940 & 0.000 & 0.922 & 0.000 \\ 0.000 & 0.000 & 0.000 & 1.000 & 0.000 \\ 0.017 & -170.612 & 0.000 & -7.853 & 0.000 \\ 0.000 & -12.000 & 12.000 & 0.000 & 0.000 \end{bmatrix} \begin{bmatrix} V_T \\ \alpha \\ \theta \\ q \\ h \end{bmatrix} + \begin{bmatrix} 6.741 & -0.006 & -0.006 \\ -0.090 & -0.008 & -0.008 \\ 0.000 & 0.000 & 0.000 \\ 0.000 & -1.328 & -1.328 \\ 0.000 & 0.000 & 0.000 \end{bmatrix} \begin{bmatrix} \delta_{th} \\ \delta_{ev}^R \\ \delta_{ev}^L \end{bmatrix} \quad (5)$$

Lateral-directional dynamics

$$\begin{bmatrix} \dot{\beta} \\ \dot{\phi} \\ \dot{\psi} \\ \dot{p} \\ \dot{r} \end{bmatrix} = \begin{bmatrix} -0.072 & 0.807 & 0.000 & 0.159 & -0.987 \\ 0.000 & 0.000 & 0.000 & 1.000 & 0.161 \\ 0.000 & 0.000 & 0.000 & 0.000 & 1.013 \\ -115.511 & 0.000 & 0.000 & -10.254 & 1.445 \\ -15.179 & 0.000 & 0.000 & -0.023 & -0.233 \end{bmatrix} \begin{bmatrix} \beta \\ \phi \\ \psi \\ p \\ r \end{bmatrix} + \begin{bmatrix} 0.000 & 0.000 & 0.000 \\ 0.000 & 0.000 & 0.000 \\ 0.000 & 0.000 & 0.000 \\ 0.000 & -0.930 & 0.930 \\ 0.000 & -0.132 & 0.132 \end{bmatrix} \begin{bmatrix} \delta_{th} \\ \delta_{ev}^R \\ \delta_{ev}^L \end{bmatrix} \quad (6)$$

where δ_{th} is a throttle level. Dynamic properties of BWB UAV are summarized in Table 3. From Table 3, we can observe that it shows a specific property of BWB configuration as mentioned in Introduction, i.e its short period mode is fast and the damping ratio is comparatively small. Unfortunately, also it has an unstable dutch-roll mode, we suppose, which is caused by the fact that there is no appropriate control surface such as rudder to damp out yawing oscillation even though it has a swept-back wing.

Autopilot design

Using the linear dynamic mode in Eqs. (5) and (6) and considering the dynamic properties shown in Table 3, autopilot for longitudinal and lateral-directional motions is designed by applying the classical approach referred to Ref. [9]. As shown in Fig. 5, longitudinal autopilot is composed of speed controller and altitude hold controller which is integrated with the inner-loop controllers for pitch attitude stabilization and orientation. Lateral-directional autopilot is for heading orientation constituted of the inner-loop controller for roll stabilization and orientation as illustrated in Fig. 6. The gains in the dotted line of Figs. 5 and 6 are for determining the direction of deflection of each elevon. The designed controllers for autopilot of BWB UAV are summarized in Table 4 and the bode diagrams of altitude hold and heading orientation control loop are shown in Fig. 7. The results shown in Fig. 7 present that the designed autopilot system assures a sufficient gain margin and phase margin.

Table 4. Controllers for Autopilot of BWB UAV

Speed Control Loop	Altitude Hold Loop	Heading Orientation Loop
$G_{VT}(s) = \frac{0.4s + 0.12}{s}$	$K_q = 8.0$	$K_p = 10.0$
	$G_\theta(s) = \frac{5.0s + 2.5}{s}$	$G_\theta(s) = \frac{5.0s + 1.2}{s}$
	$G_h(s) = \frac{0.05s + 0.01}{s}$	$G_\psi(s) = 2.5$

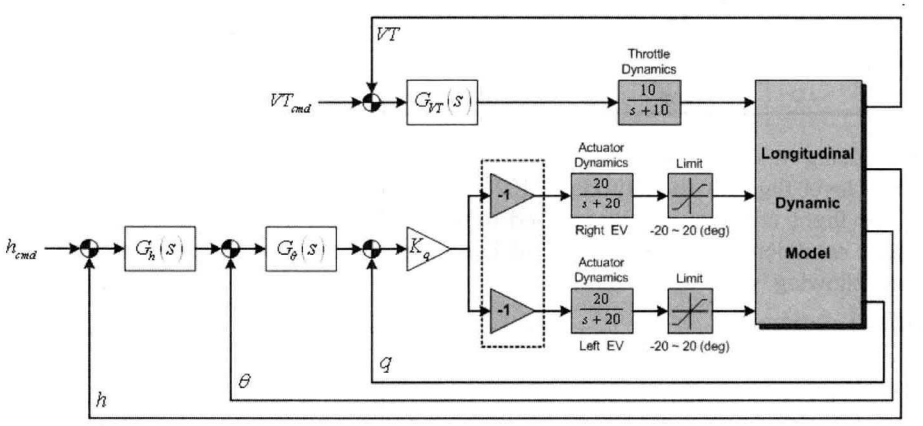

Fig. 5. Autopilot Structure for Longitudinal Motion

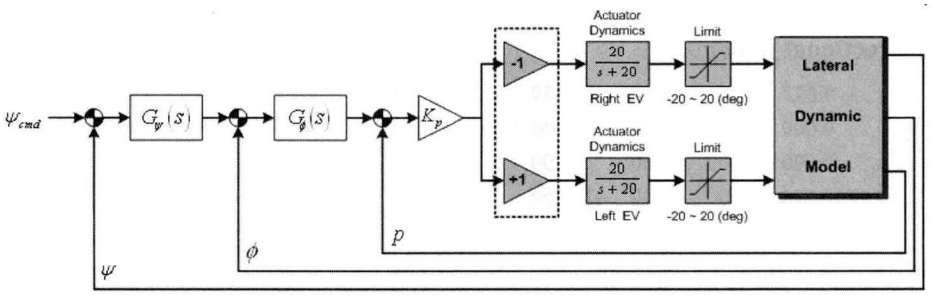

Fig. 6. Autopilot Structure for Lateral-directional Motion

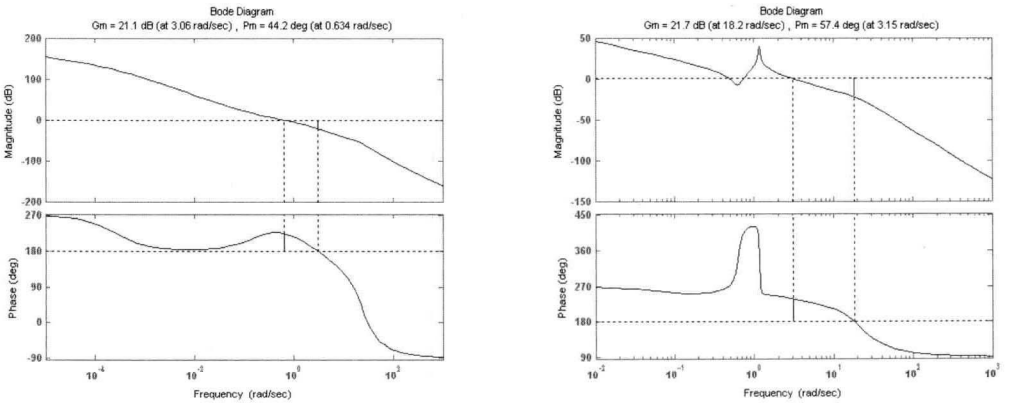

Fig. 7. Bode Diagrams : Altitude Hold Loop (Left) and Heading Orientation Loop (Right)

Performance evaluation of autopilot for BWB UAV

Since the 6-DOF motions of BWB UAV are controlled by only one pair of control surface, i.e. elevon, control allocation technique, which distributes the demanded control signal to each control surface, necessitates to effectively merge the longitudinal and lateral-directional autopilot. There are several researches related to applying control allocation scheme to control of BWB aircraft [7, 11-13], however, we distribute the control signals produced by longitudinal and lateral-directional autopilot to right and left elevon by using a simple distributor as shown in Fig. 8. Fig. 9 shows the control performance of the designed autopilot when the step input command of altitude and heading angle is simultaneously imposed. Here, we can observe that the performance of heading orientation loop is poor compared to altitude hold loop. In fact, to improve this control performance of the designed autopilot, optimal control allocator should be designed and integrated into this autopilot system. Also, the right and left control surfaces are actuated showing an asymmetric trends during the initial transient period to achieve the control objective of longitudinal and lateral-directional autopilot loops.

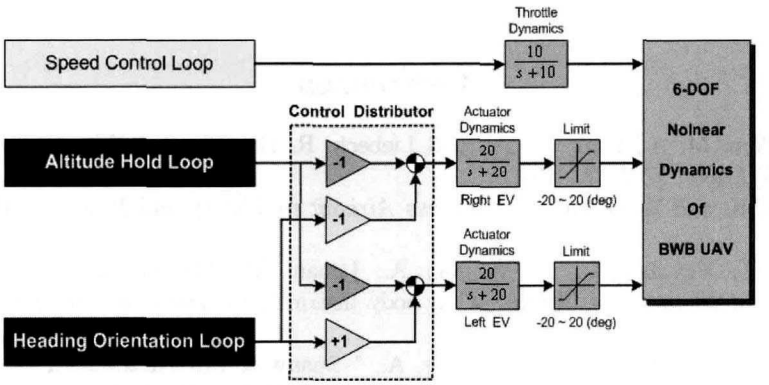

Fig. 8. The Illustration of Simple Control Distributor for Autopilot of BWB UAV

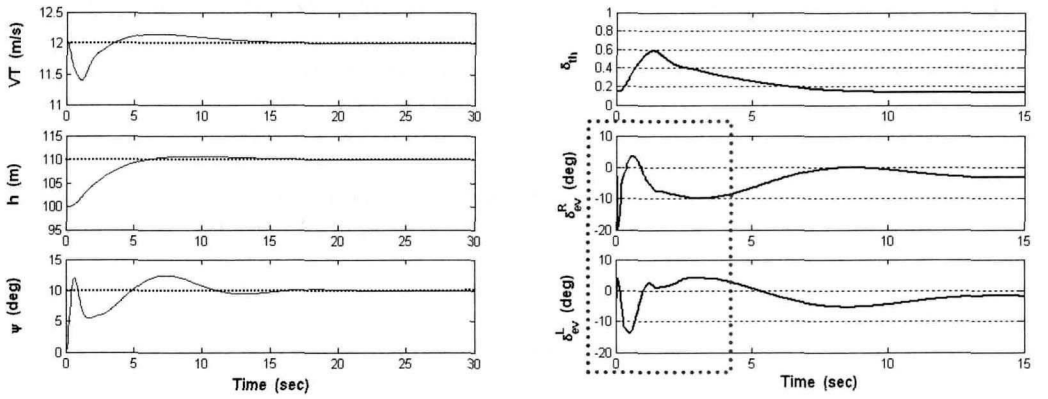

Fig. 9. The Performances of Autopilot of BWB UAV

Conclusions

In this paper, the modeling and autopilot design procedure of BWB UAB are described. The static and dynamic stability derivatives and control derivatives required for aerodynamic modeling are obtained by using the software of 'Digital DATCOM'. Based on the 6-DOF equations of motion

of BWB UAV and its nonlinear simulation model, we calculate the trim condition and a set of linearized model of a particular reference flight condition. The linearized model provided the specific flying characteristics of BWB UAV, such as high frequency and slightly less damped short period mode and unstable dutch-roll mode, generally not being shown in the conventional type of fixed-wing UAV. Finally, the autopilot for speed control, altitude hold, and heading orientation was designed and evaluated its performance through nonlinear simulation. Although the research related to design an optimal control allocator and implement it to this BWB UAV model remains further study, we constituted a simple control distributor to effectively merge the longitudinal and lateral-directional autopilot. Since only one pair of control surface, i.e. elevon, is actuated to simultaneously control for longitudinal and lateral-directional motion, a control allocation technique to distribute the demanded control signals to each control surface is essential for BWB UAV.

Acknowledgement

The authors gratefully acknowledge for financial support by Korea Ministry of Knowledge Economy.

References

1. Portsdam, M. A., Page, M. A., and Liebeck, R. H., "Blended Wing Body Analysis and Design", *AIAA Paper* 97-2317, 1997.

2. Nickel, K. and Wohlfahrt, M., *Tailless Aircraft in Theory and Practice*, AIAA Education Series, 1994.

3. Qin. N., Vavalle, A., Le Moigne, A., Laban, M., Hackett, K., and Weinerfelt, P., "Aerodynamic consideration of blended wing body aircraft", *Progress in Aerospace Science*, Vol. 40, pp. 321-343, 2004.

4. Qin, N., Vavalle, A., and Le Moigne, A., " Spanwise Lift Distribution for Blended Wing Body Aircraft", *Journal of Aircraft*, Vol. 42, No. 2, pp. 356-365, Mach-April 2005.

5. Berends, J. P. T. J., Van Tooren, M. J. L., and Belo, D. N. V., "A Distributed Multi-Disciplinary Optimization of a Blended Wing Body UAV using a Multi-Agent Task Environment", *47th AIAA/ASME/ASCE/AHS/ASC Structures, Structural Dynamics, and Materials Conference*, Newport, Rhode Island, May 2006.

6. Lee, D. S., Gonzalez, L. F., Auld, D. J., and Wong, K. C., "Aerodynamic Shape Optimization of Unmanned Aerial Vehicles using Hierarchical Asynchronous Parallel Evolutionary Algorithms", *International Journal of Computational Intelligence Research*, Vol. 3, No. 3, pp. 231-252, 2007.

7. Jung, D. W. and Lowenberg, M. H., " Stability and Control Assessment of a Blended-Wing-Body Airliner Configuration", *AIAA Atmospheric Flight Mechanics Conference and Exhibit*, San Francisco, California, Aug. 2005.

8. Donlan, C. J., " An interim report on the stability and control of tailless airplanes", *NACA Report No. 796*, Aug. 1944.

9. Stevens, B. L. and Lewis, F. L., *Aircraft Control and Simulation*, John Wiley & Sons, Inc., New York, 1992.

10. _____, *The USAF Stability and Control DATCOM Volume 1, Users Manual*, McDonnell Douglas Astronautics Company, April 1979

11. Buffington, J. M., "Tailless Aircraft Control Allocation", *AIAA Paper 97-3605*, 1997.

12. Bieniawski, S. R., Kroo, I. M., and Wolpert, D. H., "Flight Control with Distributed Effectors", *AIAA Guidance, Navigation, and Control Conference and Exhibit*, Aug. 2005, San Francisco, California, 2005.

13. Haitao, W. and Jinyuan, G., "Trajectory tracking control for uninhabited air vehicles", *IEEE CIMCA-IAWTIC'06*, 2006.